

# Angle-resolved photoemission spectroscopy of superconducting LiFeAs: Evidence for strong electron-phonon coupling

A. A. Kordyuk,<sup>1,2</sup> V. B. Zabolotnyy,<sup>1</sup> D. V. Evtushinsky,<sup>1</sup> T. K. Kim,<sup>1</sup> I. V. Morozov,<sup>1,3</sup> M. L. Kulić,<sup>4</sup> R. Follath,<sup>5</sup> G. Behr,<sup>1</sup> B. Büchner,<sup>1</sup> and S. V. Borisenko<sup>1</sup>

<sup>1</sup>*Institute for Solid State Research, IFW-Dresden, PO Box 270116, D-01171 Dresden, Germany*

<sup>2</sup>*Institute for Metal Physics, The National Academy of Sciences of Ukraine, 03142 Kyiv, Ukraine*

<sup>3</sup>*Moscow State University, Moscow 119991, Russia*

<sup>4</sup>*Institute for Theoretical Physics, Goethe University, D-60438 Frankfurt am Main, Germany*

<sup>5</sup>*Helmholtz-Zentrum Berlin, BESSY, D-12489 Berlin, Germany*

(Received 24 February 2011; published 15 April 2011)

By applying a state-of-the-art angle-resolved photoemission to LiFeAs, the only stoichiometric pnictide superconductor without magnetic ordering, we identify a clear fingerprint of the phonon spectrum in the fermionic self-energy and estimate the electron-phonon coupling strength, which appears to be sufficient to mediate the superconductivity. This result suggests that the superconductivity in pnictides could be based on the conventional phonon pairing enhanced by the van Hove singularity in the electronic density of states and by the strong electron-electron interaction.

DOI: [10.1103/PhysRevB.83.134513](https://doi.org/10.1103/PhysRevB.83.134513)

PACS number(s): 74.70.Xa, 74.20.Fg, 74.25.Kc, 79.60.-i

## I. INTRODUCTION

The ability of phonons to mediate high-temperature superconductivity<sup>1</sup> has been highly debated since the initial discovery of the superconducting cuprates, but has remained uncertain until now. In particular, the question about a pairing glue has been difficult to answer, since experimental evidence has been provided for both the phonons<sup>2</sup> and the spin fluctuations.<sup>3</sup> The iron-based pnictides, a newly discovered family of high- $T_c$  superconductors, seem to provide a clear case where the phonons definitely lose to spin fluctuations in the nomination for the most-expected pairing glue, because many of the previous estimates have suggested that the electron-phonon coupling in ferropnictides is by far insufficient to mediate the pairing.<sup>4,5</sup> To confirm such conclusions, the experimental determination of the role of phonons and spin fluctuations in pnictides is required.

The fermionic self-energy, the distribution of which in the momentum-energy space can be measured by angle-resolved photoemission spectroscopy (ARPES), is the first quantity to look for fingerprints of the interaction responsible for the superconducting pairing.<sup>6</sup> Such an idea has been applied to superconducting cuprates,<sup>3,7-9</sup> but its direct application to pnictides was not possible due to the essential three-dimensionality of the electronic band structure<sup>10</sup> and magnetic ordering.<sup>11</sup> In this paper, we report the investigation of the fermionic self-energy in LiFeAs, which may become a key compound for the pnictide puzzle since it does not show any static magnetic ordering, but has a rather high critical temperature ( $T_c = 18$  K) (Refs. 12–14) and a sizable isotropic superconducting gap with  $2\Delta/kT_c = 4$ .<sup>15,16</sup> From an experimental point of view, LiFeAs provides a simplest case among the other pnictides for the following reasons. First, it is a stoichiometric compound that exhibits superconductivity at ambient pressure without chemical doping,<sup>12-14</sup> thus it can be easily studied by the experimental techniques which require clean samples without impurities. Second, it reveals a

perfectly two-dimensional Fe- $3d_{xy}$  electronic band,<sup>15,17,18</sup> well separated in momentum space from other bands, which makes it possible to precisely derive the quasiparticle self-energy<sup>9</sup> from ARPES spectra and analyze its fine structure.<sup>19,20</sup> Finally, LiFeAs cleaves between the two layers of Li atoms resulting in equivalent and neutral counterparts,<sup>21</sup> offering a unique opportunity to overcome the problem of polar surface that can be crucial for the surface-sensitive methods.<sup>22</sup>

## II. EXPERIMENT AND RESULTS

ARPES experiments have been performed at the “1<sup>3</sup>” beamline at BESSY equipped with an SES 4000 analyzer and <sup>3</sup>He cryo-manipulator, with the lowest temperature on the sample below 0.9 K. The spectra for the analysis of the dispersion and scattering-time anomalies have been measured along several cuts (cuts 1 and 2 in Fig. 1), the position of which in the reciprocal space and excitation energy have been optimized for the maximum of photoemission intensity at 4 meV, and 0.01 Å<sup>-1</sup> of the energy and momentum resolution, respectively. Cut 3 has been resampled from the map. The experimental statistics in this cut (~40 counts per pixel) is 20–40 times lower, but still sufficient to measure the width of the momentum distribution curves (MDCs)<sup>23</sup> down to -0.1 eV, and determine the width of the energy distribution curves (EDCs) at the bottom of the band at about -0.2 eV.

Figure 1(a) presents the Fermi surface map of LiFeAs, where the band of interest is contoured by the dotted line. The systematic ARPES study of this band<sup>15</sup> shows that it is really strongly two-dimensional: neither its position nor width vary with excitation energy and polarization. Figure 1 also shows the ARPES images, i.e., the cuts of the photoemission intensity in momentum-energy space: the spectra in (c) and (d) were measured with ultimate experimental resolution and statistics and used to extract the fermionic self-energy (the mass enhancement and the quasiparticle lifetime) and analyze its fine structure; (b) shows the cut obtained by resampling

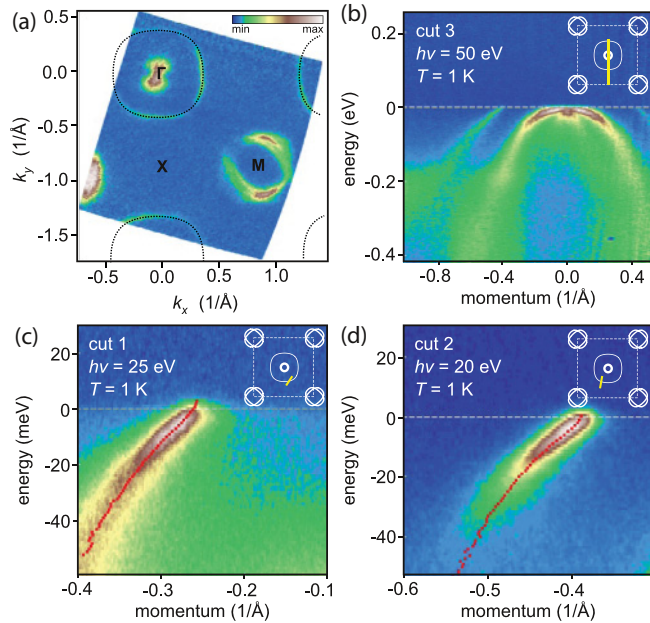


FIG. 1. (Color online) (a) The Fermi surface (FS) map of LiFeAs: the thinnest contour around the  $\Gamma$  point (dotted line) corresponds to the hololike FS sheet, which is formed by the two-dimensional band formed by Fe- $3d_{xy}$  orbitals. (b–d) Different cuts of this band. The position of each cut is shown in the insets. Red squares on (c) and (d) trace the experimental dispersion.

the map data, from which we can estimate the behavior of the self-energy on the energy scale of the bandwidth.

### III. DATA ANALYSIS

Extracting the self-energy from ARPES spectra is, in general, a nontrivial problem which requires certain assumptions (see Ref. 20 and references therein). Nevertheless, one can reveal the structure of the underlying bosonic spectrum analyzing the details of MDC dispersion or MDC width for a strongly dispersing band. On the other hand, one can estimate the value of the scattering rate directly from the EDC width for a weakly dispersing band. For the Fe- $3d_{xy}$  band, which in LiFeAs is well separated from other bands in  $k\omega$  space, we can combine both the MDC and EDC analysis.

#### A. Multiple phonon modes from MDC dispersion

Figure 2(a) shows the experimental dispersions, i.e., the positions of the MDC maxima as a function of energy, for cuts 1 and 2. Except for a tiny effect of the superconducting gap in the close vicinity ( $\sim 3$  meV) of the Fermi level, the variation of band dispersion with temperature is negligible. Importantly, all the dispersions reveal three sharp kinks. Such kinks in the experimental dispersion are usually a consequence of the interaction of the electrons with sharp modes residing at the kink energies in a bosonic spectrum.<sup>7–9,19,20</sup> All three kinks are clearly seen on the temperature-integrated and smoothed-dispersion curve (solid yellow curve), the straight segments of which are highlighted by the dotted lines. Taking the second derivative of this dispersion (dotted yellow curve in the inset) reveals the kink positions in a form of clear peaks.

The energies of the observed kinks are remarkably close to the energies of the optical-phonon modes (indicated by the vertical dashed lines): 15, 30, and 44 meV, recently calculated for this compound.<sup>5</sup> The lowest kink corresponds to the lowest phonon mode ( $121 \text{ cm}^{-1} E_g$ ) and the highest kink corresponds to the highest mode ( $356 \text{ cm}^{-1} A_{1g}$ ), while the middle kink fits to the energy of one of the intermediate phonon modes such as  $240 \text{ cm}^{-1} E_g$ .<sup>5</sup>

#### B. Bosonic spectrum from MDC width

Now we turn to the quasiparticle scattering rate, or the imaginary part of the self-energy  $\Sigma''$ , which is inversely proportional to the quasiparticle lifetime. Observing such a clear fingerprint of the bosonic spectrum in the experimental dispersion, the fine structure of which is entirely associated with the real part of the self-energy, one should expect to see a very similar structure in its imaginary part.

In principle, the scattering rate is an even more appropriate quantity to look for the details of the bosonic spectrum, since their relation is much simpler. Indeed, for a momentum-independent phonon (generally, boson) spectrum  $F(\Omega)$  and electron-phonon coupling  $\alpha$ , the phononic contribution to the imaginary part of the quasiparticle self-energy can be written as<sup>3</sup>

$$\Sigma''(\omega) \propto \int_{-\infty}^{\infty} \alpha^2 F(\Omega) K(\omega, \Omega) N(\omega - \Omega) d\Omega, \quad (1)$$

where  $K(\omega, \Omega) = n(\Omega) + f(\omega - \Omega)$ ,  $n$  and  $f$  stand for the Bose and Fermi functions, respectively, and  $N(\omega)$  is the density of electronic states (DOS). Then, for  $N(\omega) = \text{const}$ , and zero temperature, we have

$$\frac{d\Sigma''(\omega)}{d\omega} \propto \alpha^2 F(\omega). \quad (2)$$

So, in the most trivial case of isotropic electron-boson coupling, constant DOS, and zero temperature, the bosonic spectrum simply coincides with the differential scattering rate. Until the width of the peaks in  $\alpha^2 F(\Omega)$  remains much smaller than the width of DOS anomalies, their positions should not deviate noticeably from the positions of the peaks in  $d\Sigma''/d\omega$ .

The real and imaginary parts of  $\Sigma$  are related by the Kramers-Kronig transform (see Ref. 20 for the examples of  $\Sigma$  parts in cuprates). This generally means that in order to derive  $\alpha^2 F$  from  $\Sigma'$ , one needs to solve an Eliashberg-type equation.<sup>6,19</sup> Nevertheless, for the presented accuracy, the corresponding peak positions in  $d\Sigma''/d\omega$  and  $d^2\Sigma'/d\omega^2$  coincide.<sup>19,20</sup> So, the second derivative of the MDC dispersion, though not revealing the true profile of  $\alpha^2 F(\Omega)$ , still gives a good estimate for the positions of the peaks in the bosonic spectrum.

In Fig. 2(b), we show the MDC width  $\Delta k$ , which is simply proportional to  $\Sigma''$ ,<sup>20</sup> along the same two cuts over the same energy range as in Fig. 2(a). The first derivatives of integrated  $\Delta k(\omega)$  dependences, shown in the inset, reveal the bosonic spectrum that is peaked at the same frequencies (slight displacements of the highest modes from 44 meV is a natural influence of the noise, which highly increases with binding energy) and is remarkably similar to the phonon density of states derived from the phonon dispersions calculated in Ref. 5.

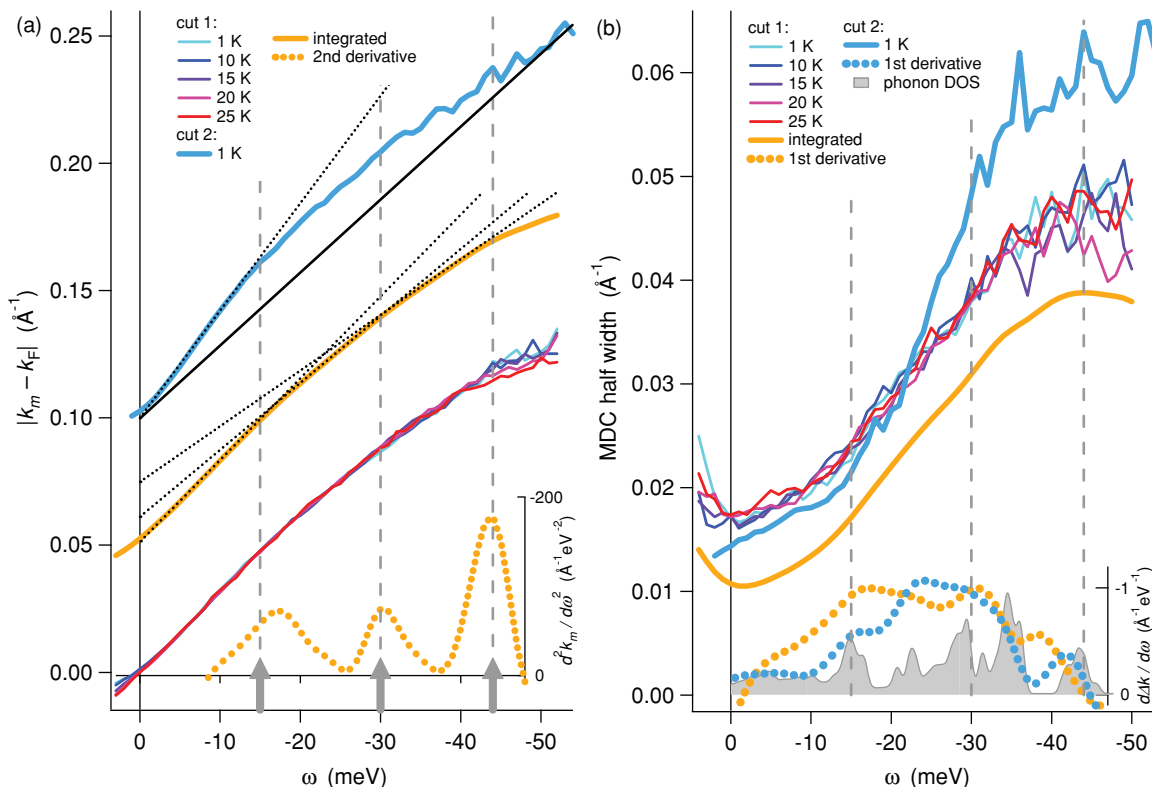


FIG. 2. (Color online) Fingerprints of low-energy interaction. Experimental (or renormalized) dispersions: (a) The positions of MDC maxima  $k_m$  as a function of energy  $\omega$  for cut 1 at different temperatures, for the same cut but temperature integrated and smoothed, and for cut 2. The last two curves are shifted up by 0.05 and 0.1  $\text{\AA}^{-1}$ , respectively. The inset shows the second derivative of the dispersion vs the same energy axis. (b) MDC width (the half-width at half maximum) which is proportional to the inversed lifetime of the fermionic quasiparticles. The similarly integrated curve is shifted down. The inset shows the differential scattering rates for cuts 1 and 2 on top of the phonon density of states derived from Ref. 5. On both panels, the vertical dashed lines indicate the positions of three optical-phonon modes: 15 meV (the lowest one), 30 meV, and 44 meV (the highest one).

### C. Coupling strength from MDC dispersion

The contribution to the quasiparticle scattering rate of the phonon spectrum, which is confined below 44 meV, should saturate above that energy. This is exactly the case as one can see in Fig. 2(b). Since the real part of the self-energy rapidly decreases below the cutoff of the phonon spectrum, we can neglect its contribution to the total renormalization soon after this energy, and estimate the phonon coupling constant from the dispersion curves  $\varepsilon(k)$ . Formally, this can be done if the band velocity can be defined simultaneously by two equations:  $v = d\varepsilon/dk = \varepsilon/(k - k_F)$ . The dotted and solid lines on the dispersion curve from cut 2 in Fig. 2(a) represent the low-energy experimental dispersion (that includes the renormalization by phonons) and the dispersion as it would be without coupling to phonons. Their velocities are  $v_L = 0.24 \text{ eV}\text{\AA}$  and  $v_H = 0.35 \text{ eV}\text{\AA}$ , respectively, and, assuming that the velocity of the phonon undressed band does not change much in this energy range, the value  $\tilde{\lambda}_{\text{ph}} = v_H/v_L - 1 = 0.46$  gives an electron-phonon coupling strength renormalized by other nonphononic interactions, as discussed below.

In order to show that the phonon undressed dispersion can indeed be considered as linear in the region of interest, we approximate it by the cosine function that goes through the bottom of the measured band and the Fermi crossing  $k_F$ ,

as shown in Fig. 3. This is in line with the aforementioned assumption that the effect of renormalization by phonons can be neglected below  $-50 \text{ eV}$ . One can see that the region of interest (between 0.38 and 0.55  $\text{\AA}^{-1}$ ) is in the middle of the band, so the change of the band velocity in this range can be neglected: Even the change of the band velocity between the Fermi level and  $-50 \text{ meV}$ , where  $v$  is maximal (the corresponding momenta refer to vertical lines 1 and 2, respectively), is less than 5%, which is certainly within the accuracy of the estimates made in this paper. Moreover, for the actual momenta at which  $v_L$  and  $v_H$  are determined (shown by lines 1 and 3, respectively), the effect of nonlinearity is even less, i.e., within 3%.

### D. Self-energy scale and EDC width

Can the electron-phonon interaction, which we have identified and evaluated, be responsible for the strong (factor of 3) renormalization of the bandwidth?<sup>15</sup> Evidently not, since its contribution to the quasiparticle self-energy is confined within the energy range of phonons (44 meV). In order to understand the missing mechanism for the strong renormalization, in Fig. 4 we show an overview plot of the scattering rate in LiFeAs on the scale of the bandwidth and compare it

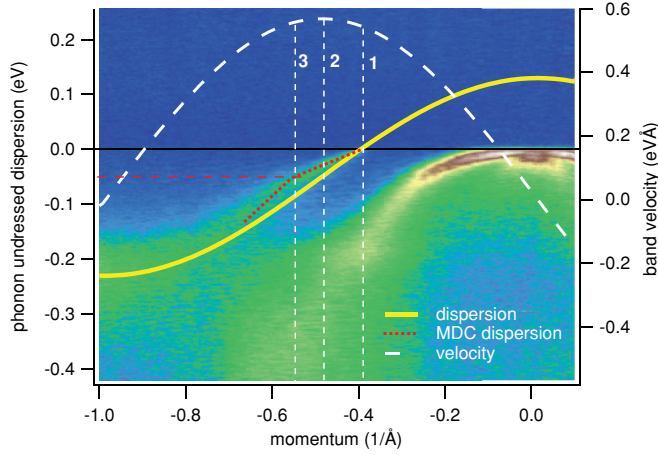


FIG. 3. (Color online) An estimate of the phonon undressed dispersion of the Fe- $3d_{xy}$  band and the corresponding band velocity.

to the same quantity measured along the nodal direction in a cuprate superconductor, that is, the optimally doped  $(\text{Bi,Pb})_2\text{Sr}_2\text{Ca}_2\text{CuO}_{8-\delta}$  (BSCCO).<sup>8</sup> The relation of the MDC width with  $\Sigma''$  and quasiparticle lifetime  $\tau$  is simple:  $\hbar/\tau = \Sigma'' = v_F \Delta k$ , provided the Fermi velocity of the bare electrons  $v_F$  is known.<sup>20</sup> Taking here  $v_F \approx 1 \text{ eV}\text{\AA}$ ,<sup>15,17,18</sup> we add the energy scale as the right axis to Fig. 4.

From the overview plot, one can see that the phonons are not the only contributors to the scattering rate. The phonon-related step develops on a background of another contribution, which shows linear dependence on energy both below (as indicated by the blue dashed line in Fig. 4) and above the phonon energy range, and tends to saturate above 100 meV so that the total scattering rate reaches  $\sim 80 \text{ meV}$ . The saturated value of  $\Sigma''$  can be estimated from the band broadening at its very bottom [see Fig. 1(b)], where the EDC half-width gives the same 80 meV.

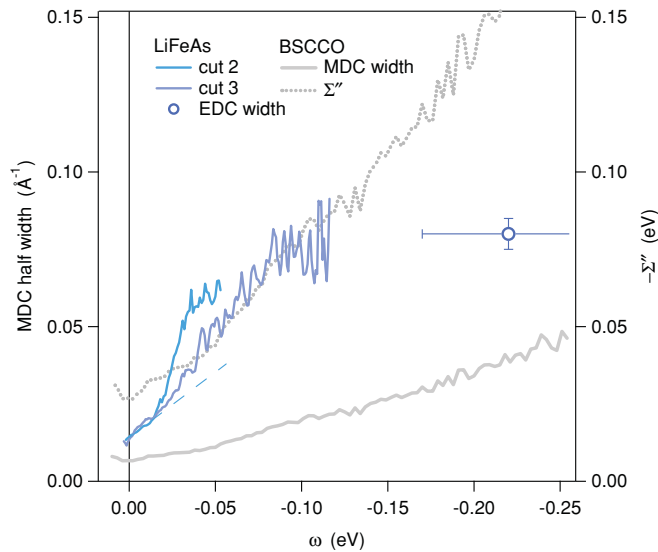


FIG. 4. (Color online) Scattering rate on large-energy scale. MDC width and the imaginary part of fermionic self-energy for the cuts 1 and 2. MDC width for  $(\text{Bi,Pb})_2\text{Sr}_2\text{Ca}_2\text{CuO}_{8-\delta}$  (BSCCO)<sup>8</sup> is shown for comparison. The EDC width at the bottom of the band and the imaginary part of the self-energy for BSCCO refer to the right axis.

This is shown in Fig. 4 by the circle (the horizontal error bars represent the uncertainty in  $\Sigma''$ ). This is independent evidence that  $1 \text{ eV}\text{\AA}$  is a good estimate for  $v_F$ , and, consequently, that the renormalization factor of 3 in LiFeAs is caused mainly by the nonphonon scattering channel, which is natural to associate with an electron-electron scattering<sup>8</sup> with  $\lambda_{\text{el}} = 2$ .

## IV. DISCUSSION

### A. “Bare” electron-phonon coupling

Now one can estimate the “bare” electron-phonon coupling  $\lambda_{\text{ph}}$ . Assuming that the self-energy contributions are additive, then total  $\lambda = \lambda_{\text{ph}} + \lambda_{\text{el}}$ .<sup>24</sup> From the definitions of  $\lambda = v_F/v_L - 1$ ,  $\lambda_{\text{el}} = v_F/v_H - 1$ , and  $\tilde{\lambda}_{\text{ph}}$ , we have

$$\lambda_{\text{ph}} = \frac{v_F}{v_L} - \frac{v_F}{v_H} = (1 + \lambda_{\text{el}})\tilde{\lambda}_{\text{ph}}. \quad (3)$$

So,  $\lambda_{\text{ph}} = 1.38$  and  $\tilde{\lambda}_{\text{ph}} = 0.46$  give the strength of the coupling to phonons of the bare electrons and the electrons renormalized by the electron-electron interaction,<sup>6</sup> respectively. Both the values are essentially larger than the calculated  $\lambda_{\text{ph}}^{\text{calc}} = 0.29$ ,<sup>5</sup> though it is  $\lambda_{\text{ph}}$  that seems more reasonable to compare to  $\lambda_{\text{ph}}^{\text{calc}}$ .

### B. Superconducting transition temperature

Based on small  $\lambda_{\text{ph}}^{\text{calc}}$  and on the McMillan’s formula<sup>25</sup> for  $T_c$  modified by Allen and Dynes,<sup>26</sup>

$$T_c = \frac{\omega_D}{1.2} \exp \left[ -\frac{1.04(1 + \lambda)}{\lambda - \mu^*(1 + 0.62\lambda)} \right], \quad (4)$$

there is an opinion that the phonon coupling in LiFeAs is by far not sufficient to explain the onset of superconductivity at 18 K.<sup>5</sup> So, it is interesting to reevaluate the  $T_c$  with the experimental estimates for  $\lambda_{\text{ph}}$  in hand.

Although which parameter,  $\tilde{\lambda}_{\text{ph}}$  or  $\lambda_{\text{ph}}$ , is more relevant here is not straightforward,<sup>6,24</sup> the direct substitution of both values in this formula (keeping the same  $\omega_D = 100 \text{ K}$  and  $\mu^* = 0.13$ ) increases  $T_c$  from 0.005 to 0.5 and 10 K, respectively. It is worth mentioning that substitution of the renormalized value  $\tilde{\lambda}_{\text{ph}}$  into the original BCS formula,<sup>27</sup>

$$T_c = 1.14\omega_D \exp \left( -\frac{1}{\lambda} \right), \quad (5)$$

with the same  $\omega_D$ , gives  $T_c = 13 \text{ K}$ .

Based on the extensive studies of the limitations of the McMillan’s formula and its modifications,<sup>1,28–30</sup> it is easy to assume that the remaining difference will be eliminated by taking into account the real spectrum of phonons,<sup>28</sup> real electronic density of states,<sup>29–31</sup> and the intraband electron-boson scattering.<sup>32</sup> While the evaluation of the contributions of each of those mechanisms toward the further increase of the  $T_c$  waits for the numerical solution of the Eliashberg equation, our study suggests that the electronic band structure itself plays an important role. The linear electron-electron scattering rate (see Fig. 4) is a well-known signature of an extended van Hove singularity (vHs) residing at the Fermi level.<sup>30</sup> The extended vHs is, in fact, observed as a flattening of the other band at the Fermi level in the center of the Brillouin zone [Fig. 1(b)], as discussed in detail in Ref. 15. The ability of vHs to increase

the critical temperature considerably is well known and has been discussed extensively for the cuprates.<sup>29–31</sup>

### C. Electron-electron interaction

An evident reason for a much larger value of  $\lambda_{\text{ph}}$ , compared to the theoretical estimates, is that the fermionic DOS is higher than expected. Since the two mechanisms of the DOS enhancement, the strong renormalization and the vHs, seem to be common for the pnictides,<sup>15,33</sup> resolving their microscopic origin can be a key to solving the problem of superconductivity in these compounds.

Besides the straightforward Coulomb interaction,<sup>6</sup> there is a possibility that the observed electron-electron scattering is dominated by electron coupling to the spin fluctuations, which are generally expected to be strong in all the ferropnictides<sup>34</sup> and have been reported in LiFeAs by NMR study.<sup>35,36</sup> If the spin fluctuations are really strong in LiFeAs, they can help to increase the  $T_c$  either indirectly, contributing to the DOS enhancement, or by providing another nonphonon mechanism for the superconducting pairing.<sup>34,37</sup>

### V. SUMMARY

We have observed and identified the fingerprints of the phonon spectrum both in the experimental dispersion and in the lifetime of fermionic quasiparticles associated with the Fe-

$d_{xy}$  band of LiFeAs. The estimated electron-phonon coupling strength is found to be substantially larger than the calculated one,<sup>4,5</sup> as well as those derived from recent optical pump-probe experiments,<sup>38,39</sup> and even those that can be estimated for the cuprates assuming that the nodal kink there is formed solely by phonons.<sup>2</sup> Since similar electron-phonon coupling is expected for all the pnictides, this suggests an important role of phonons for the mechanism of pairing in these compounds. One may note that the determined  $\lambda_{\text{ph}}$  is in the intermediate crossover region, where the extended vHs, enhanced DOS, and high  $T_c$  could be also explained by the strong-coupling polaronic superconductivity.<sup>40</sup> On the other hand, the strong electron-electron coupling, for which the evidence in the fermionic lifetime is also present, suggests that the spin fluctuations may play an important role in increasing  $T_c$  to even higher values.

### ACKNOWLEDGMENTS

We acknowledge discussions with I. Mazin, A. Yaresko, I. Eremin, S.-L. Drechsler, T. Dahm, A. S. Alexandrov, and E. Pashitskii. The project was supported by the DFG under Grants No. KN393/4, No. BO 1912/2-1, No. BE1749/13, No. 486RUS 113/982/0-1, and No. SPP 1458. I.V.M. also acknowledges support from the Ministry of Science and Education of the Russian Federation (Contract No. P-279) and by RFBR-DFG (Project No. 10-03-91334).

<sup>1</sup>V. L. Ginzburg and D. A. Kirzhnits, *High-temperature Superconductivity* (Consultants Bureau, New York, 1982).

<sup>2</sup>T. P. Devereaux, T. Cuk, Z.-X. Shen, and N. Nagaosa, *Phys. Rev. Lett.* **93**, 117004 (2004).

<sup>3</sup>T. Dahm, V. Hinkov, S. V. Borisenko, A. A. Kordyuk, V. B. Zabolotnyy, J. Fink, B. Buchner, D. J. Scalapino, W. Hanke, and B. Keimer, *Nature Phys.* **5**, 217 (2009).

<sup>4</sup>L. Boeri, O. V. Dolgov, and A. A. Golubov, *Phys. Rev. Lett.* **101**, 026403 (2008).

<sup>5</sup>R. A. Jishi and H. M. Alyahyaei, *Adv. Condens. Matter Phys.* **2010**, 804343 (2010).

<sup>6</sup>See, e.g., D. J. Scalapino, in *Superconductivity*, edited by R. D. Parks (Marcel Dekker, New York, 1969), p. 449.

<sup>7</sup>X. J. Zhou, J. Shi, T. Yoshida, T. Cuk, W. L. Yang, V. Brouet, J. Nakamura, N. Mannella, S. Komiyama, Y. Ando, F. Zhou, W. X. Ti, J. W. Xiong, Z. X. Zhao, T. Sasagawa, T. Kakeshita, H. Eisaki, S. Uchida, A. Fujimori, Z. Zhang, E. W. Plummer, R. B. Laughlin, Z. Hussain, and Z.-X. Shen, *Phys. Rev. Lett.* **95**, 117001 (2005).

<sup>8</sup>A. A. Kordyuk, S. V. Borisenko, V. B. Zabolotnyy, J. Geck, M. Knupfer, J. Fink, B. Büchner, C. T. Lin, B. Keimer, H. Berger, A. V. Pan, S. Komiyama, and Y. Ando, *Phys. Rev. Lett.* **97**, 017002 (2006).

<sup>9</sup>L. Zhao, J. Wang, J. Shi, W. Zhang, H. Liu, J. Meng, G. Liu, X. Dong, W. Lu, G. Wang, Y. Zhu, X. Wang, Q. Peng, Z. Wang, S. Zhang, F. Yang, C. Chen, Z. Xu, and X. Zhou, e-print [arXiv:1002.0120](https://arxiv.org/abs/1002.0120).

<sup>10</sup>H. Q. Yuan, J. Singleton, F. F. Balakirev, S. A. Baily, G. F. Chen, J. L. Luo, and N. L. Wang, *Nature (London)* **457**, 565 (2009).

<sup>11</sup>V. B. Zabolotnyy, D. S. Inosov, D. V. Evtushinsky, A. Koitzsch, A. A. Kordyuk, G. L. Sun, J. T. Park, D. Haug, V. Hinkov, A. V. Boris, C. T. Lin, M. Knupfer, A. N. Yaresko, B. Buchner, A. Varykhalov, R. Follath, and S. V. Borisenko, *Nature (London)* **457**, 569 (2009).

<sup>12</sup>X. Wang, Q. Liu, Y. Lv, W. Gao, L. Yang, R. Yu, F. Li, and C. Jin, *Solid State Commun.* **148**, 538 (2008).

<sup>13</sup>J. H. Tapp, Z. Tang, B. Lv, K. Sasmal, B. Lorenz, P. C. W. Chu, and A. M. Guloy, *Phys. Rev. B* **78**, 060505 (2008).

<sup>14</sup>M. J. Pitcher, D. R. Parker, P. Adamson, S. J. C. Herkelrath, A. T. Boothroyd, R. M. Ibberson, M. Brunelli, and S. J. Clarke, *Chem. Commun.* **2008**, 5918 (2008).

<sup>15</sup>S. V. Borisenko, V. B. Zabolotnyy, D. V. Evtushinsky, T. K. Kim, I. V. Morozov, A. N. Yaresko, A. A. Kordyuk, G. Behr, A. Vasiliev, R. Follath, and B. Buchner, *Phys. Rev. Lett.* **105**, 067002 (2010).

<sup>16</sup>D. S. Inosov, J. S. White, D. V. Evtushinsky, I. V. Morozov, A. Cameron, U. Stockert, V. B. Zabolotnyy, T. K. Kim, A. A. Kordyuk, S. V. Borisenko, E. M. Forgan, R. Klingeler, J. T. Park, S. Wurmehl, A. N. Vasiliev, G. Behr, C. D. Dewhurst, and V. Hinkov, *Phys. Rev. Lett.* **104**, 187001 (2010).

<sup>17</sup>I. Nekrasov, Z. Pchelkina, and M. Sadovsikii, *JETP Lett.* **88**, 543 (2008).

<sup>18</sup>D. J. Singh, *Phys. Rev. B* **78**, 094511 (2008).

<sup>19</sup>J. Shi, S.-J. Tang, B. Wu, P. T. Sprunger, W. L. Yang, V. Brouet, X. J. Zhou, Z. Hussain, Z.-X. Shen, Z. Zhang, and E. W. Plummer, *Phys. Rev. Lett.* **92**, 186401 (2004).

<sup>20</sup>A. A. Kordyuk, S. V. Borisenko, A. Koitzsch, J. Fink, M. Knupfer, and H. Berger, *Phys. Rev. B* **71**, 214513 (2005).

- <sup>21</sup>A. Lankau, K. Koepf, S. Borisenko, V. Zabolotnyy, B. Buchner, J. van den Brink, and H. Eschrig, *Phys. Rev. B* **82**, 184518 (2010).
- <sup>22</sup>V. B. Zabolotnyy, S. V. Borisenko, A. A. Kordyuk, J. Geck, D. S. Inosov, A. Koitzsch, J. Fink, M. Knupfer, B. Büchner, S.-L. Drechsler, H. Berger, A. Erb, M. Lambacher, L. Patthey, V. Hinkov, and B. Keimer, *Phys. Rev. B* **76**, 064519 (2007).
- <sup>23</sup>T. Valla *et al.*, *Science* **285**, 2110 (1999).
- <sup>24</sup>See, e.g., G. Gladstone, M. A. Jensen, and J. R. Schrieffer, in *Superconductivity*, edited by R. D. Parks (Marcel Dekker, New York, 1969), p. 665.
- <sup>25</sup>W. L. McMillan, *Phys. Rev.* **167**, 331 (1968).
- <sup>26</sup>P. B. Allen and R. C. Dynes, *Phys. Rev. B* **12**, 905 (1975).
- <sup>27</sup>J. Bardeen, L. N. Cooper, and J. R. Schrieffer, *Phys. Rev.* **108**, 1175 (1957).
- <sup>28</sup>M. V. Medvedev, E. A. Pashitskii, and Y. S. Pyatiletov, *Sov. Phys. JETP* **38**, 587 (1973).
- <sup>29</sup>J. E. Hirsch and D. J. Scalapino, *Phys. Rev. Lett.* **56**, 2732 (1986).
- <sup>30</sup>P. C. Pattnaik, C. L. Kane, D. M. Newns, and C. C. Tsuei, *Phys. Rev. B* **45**, 5714 (1992).
- <sup>31</sup>R. S. Markiewicz, *J. Phys. Chem. Solids* **58**, 1179 (1997).
- <sup>32</sup>M. L. Kubic, S.-L. Drechsler, and O. V. Dolgov, *Europhys. Lett.* **85**, 47008 (2009).
- <sup>33</sup>M. Yi, D. H. Lu, J. G. Analytis, J.-H. Chu, S.-K. Mo, R.-H. He, M. Hashimoto, R. G. Moore, I. I. Mazin, D. J. Singh, Z. Hussain, I. R. Fisher, and Z.-X. Shen, *Phys. Rev. B* **80**, 174510 (2009).
- <sup>34</sup>I. I. Mazin and J. Schmalian, *Physica C* **469**, 614 (2009).
- <sup>35</sup>P. Jeglic, A. Potocnik, M. Klanjek, M. Bobnar, M. Jagodic, K. Koch, H. Rosner, S. Margadonna, B. Lv, A. M. Guloy, and D. Arcon, *Phys. Rev. B* **81**, 140511(R) (2010).
- <sup>36</sup>L. Ma, J. Zhang, G. F. Chen, and W. Yu, *Phys. Rev. B* **82**, 180501(R) (2010).
- <sup>37</sup>P. M. R. Brydon, M. Daghofer, C. Timm, and J. van den Brink, *Phys. Rev. B* **83**, 060501(R) (2011).
- <sup>38</sup>L. Stojchevska, P. Kusar, T. Mertelj, V. V. Kabanov, X. Lin, G. H. Cao, Z. A. Xu, and D. Mihailovic, *Phys. Rev. B* **82**, 012505 (2010).
- <sup>39</sup>B. Mansart, D. Boschetto, A. Savoia, F. Rullier-Albenque, F. Bouquet, E. Papalazarou, A. Forget, D. Colson, A. Rousse, and M. Marsi, *Phys. Rev. B* **82**, 024513 (2010).
- <sup>40</sup>A. S. Alexandrov, *Phys. Rev. B* **38**, 925 (1988).